on the ArgRS mechanism are being continued in this laboratory.

ACKNOWLEDGMENTS

We greatly acknowledge Professors K. E. Neet, C. L. Tsou, and S. W. Sun for critical readings of the manuscript. We thank B. Li for excellent technical assistance. We acknowledge the help of Y. Jiang for the data processing programming and Q. P. Xu for keeping the fluorometer in a very good state. We also thank X. D. Cheng for taking part in some discussion of this work.

REFERENCES

Baldwin, A. N., & Berg, P. (1966) *J. Biol. Chem. 241*, 831.
Baltzinger, M., Lin, S. X., & Remy, P. (1983) *Biochemistry 22*, 675.
Burstein, E. A. (1968) *Biofizika 13*, 433.
Char, S., & Gopinathan, K. (1986) *J. Biochem. (Tokyo) 100*, 349
Charlier, J., & Gerlo, E. (1979) *Biochemistry 18*, 3171.
Chuang, H. Y. K., & Bell, F. E. (1972) *Arch. Biochem. Biophys. 152*, 502.
Craine, J., & Peterkofsky, A. (1975) *Arch. Biochem. Biophys. 168*, 343.
Fasiolo, F., Ebel, J. P., & Lazdunski, M. (1977) *Eur. J. Biochem. 73*, 7.
Fasiolo, F., Remy, P., & Holler, E. (1981) *Biochemistry 20*, 3851.
Fersht, A. R. (1985) *Enzyme Structure and Mechanism*, W. H. Freeman, New York.
Fersht, A. R., Gangloff, J., & Dirheimer, G. (1978) *Biochemistry 17*, 3740.
Freist, W., Sternbach, H., & Cramer, F. (1981) *Eur. J. Biochem. 119*, 447.
Furlong, C. E., Morris, R. G., Krandrach, M., & Rosen, B. P. (1972) *Anal. Biochem. 47*, 514.
Godeau, J. M. (1980) *Eur. J. Biochem. 103*, 169.
Holler, E., Bennett, E. L., & Calvin, M. (1971) *Biochem. Biophys. Res. Commun. 45*, 409.
Lam, S. S. M., & Schimmel, P. R. (1975) *Biochemistry 14*, 2775.
Lefevre, J. F., Ehrlich, R., & Remy, P. (1980) *Eur. J. Biochem. 103*, 155.
Lin, S. X., Baltzinger, M., & Remy, P. (1984) *Biochemistry 23*, 4109.
Lin, S. X., Shi, J. P., Cheng, X. D., & Wang, Y. L. (1988) *Biochemistry* (preceding paper in this issue).
Mitra, S. K., & Mehler, A. H. (1967) *J. Biol. Chem. 242*, 5490.
Mitra, S. K., Chakraburtty, K., & Mehler, A. H. (1970) *J. Mol. Biol. 49*, 139.
Nazario, M., & Evans, J. A. (1974) *J. Biol. Chem. 249*, 4934.
Papas, T. S., & Peterkofsky, A. (1972) *Biochemistry 11*, 4602.
Parfait, R. (1973a) *FEBS Lett. 29*, 323.
Parfait, R. (1973b) *Eur. J. Biochem. 38*, 572.
Parfait, R., & Grosjean, H. (1972) *Eur. J. Biochem. 30*, 242.
Segel, I. H. (1975) *Biochemistry Calculations*, Wiley, New York.
Thiebe, R. (1983) *Eur. J. Biochem. 130*, 517.
Wang, H. Y., & Pan, F. (1984) *Int. J. Biochem. 16*, 1379.

Structure of a Hydroxyl Radical Induced Cross-Link of Thymine and Tyrosine†

Sam A. Margolis,*,‡ Bruce Coxon,‡ Ewa Gajewski,§ and Miral Dizdaroglu§
Center for Analytical Chemistry and Center for Chemical Physics, National Bureau of Standards, Gaithersburg, Maryland 20899

Received December 29, 1987; Revised Manuscript Received April 11, 1988

ABSTRACT: DNA–protein cross-links are formed when living cells or isolated chromatin is exposed to ionizing radiation. Little is known about the actual cross-linked products of DNA and proteins. In this work, a novel hydroxyl radical induced cross-link of thymine and tyrosine has been isolated along with a tyrosine dimer by high-performance liquid chromatography of aqueous mixtures of tyrosine and thymine that had been exposed to hydroxyl radicals generated by ionizing radiation. The isolated compounds have been examined by gas chromatography–mass spectrometry, high-resolution mass spectrometry, and ^1H and ^{13}C nuclear magnetic resonance spectroscopy. The structure of the thymine–tyrosine cross-link has been identified as the product from the formation of a covalent bond between the methyl group of the thymine and carbon 3 of the tyrosine ring. In addition, the 3,3′ tyrosine dimer was isolated and characterized. The mechanism of the formation of these compounds is discussed. This work presents the first complete chemical characterization of a hydroxyl radical induced DNA base–amino acid cross-link.

DNA–protein cross-links are formed when living cells or isolated chromatin in vitro is exposed to ionizing or UV radiation (Smith, 1976; Yamamoto, 1976; Mee & Adelstein, 1979). Although great effort has been spent on the study of this type of DNA damage, little is known about the actual cross-linked components of DNA and proteins in living cells [for a review, see Oleinick et al. (1986)]. In the case of DNA–protein cross-links in isolated chromatin, evidence indicates the involvement of hydroxyl radicals (OH radicals)[1] produced from water by ionizing radiation (Mee & Adelstein,

† This work has been supported in part by the Armed Forces Radiobiology Research Institute of the Defense Nuclear Agency, Bethesda, MD, under Research Work Unit B5103. The views expressed in this paper are those of the authors and do not reflect the official views or position of the Defense Department of the U.S. Government.

* Author to whom correspondence should be addressed.
‡ Center for Analytical Chemistry.
§ Center for Chemical Physics.

[1] Abbreviations: HPLC, high-performance liquid chromatography; GC–MS, gas chromatography–mass spectrometry; NMR, nuclear magnetic resonance; FT, Fourier transform; BSTFA, bis(trimethylsilyl)trifluoroacetamide; TSP, sodium 4,4-dimethyl-4-silapentanoate-*2,2,3,3-d*$_4$; DOPA, 3-hydroxytyrosine; NOE, nuclear Overhauser effect.

1981). Recently, OH radical induced cross-linking of a DNA base to an amino acid of a protein has been studied in model systems by use of gas chromatography–mass spectrometry (GC–MS) (Dizdaroglu, 1984; Dizdaroglu & Simic, 1985; Simic & Dizdaroglu, 1985). In the present work, OH radical induced cross-links of a model system consisting of thymine (Thy) and Tyr were isolated and studied by various analytical techniques including high-performance liquid chromatography (HPLC), GC–MS, ^1H and ^{13}C nuclear magnetic resonance (NMR) spectroscopy, and high-resolution MS. Hydroxyl radicals were generated by the application of ionizing radiation to N_2O–saturated aqueous mixtures of Thy and Tyr.

Experimental Procedures

Materials. Thymine, *o*-, *m*-, and *p*-tyrosines, and 3,4-dihydroxyphenylalanine (DOPA) were purchased from Sigma.[2] Acetonitrile, bis(trimethylsilyl)trifluoroacetamide (BSTFA), and 6 mol/L HCl were from Pierce Chemical Co., HPLC-grade acetonitrile was from J. T. Baker & Co., and water was purified through use of a MilliQ system.

Irradiations. Aqueous mixtures of thymine and tyrosine (1 mmol/L each) were saturated with N_2O for 30 min and irradiated in a ^{60}Co γ source (dose 700 Gy; dose rate 140 Gy/min). The samples were then lyophilized.

Treatment with Hydrochloric Acid. A 100-mg portion of the lyophilized material was treated with 40 mL of 6 mol/L HCl at 110 °C for 18 h in an evacuated and sealed tube. The sample was then lyophilized, redissolved in 2 mL of 0.2 mol/L HCl, and separated by HPLC. A small portion of the lyophilized sample was used for GC–MS analysis.

Trimethylsilylation. Samples were trimethylsilylated in polytetraethylene-capped Hypovials (Pierce) with 0.25 mL of a mixture of BSTFA and acetonitrile (1.5:1) by heating for 30 min at 130 °C.

Gas Chromatography–Mass Spectrometry (GC–MS). A mass-selective detector controlled by a computer work station and interfaced to a gas chromatograph was used (Hewlett-Packard). The injection port and ion source were both maintained at 250 °C, and the GC–MS interface was at 270 °C. Separations were carried out in a fused silica capillary column (15 m, 0.25-mm i.d.) coated with cross-linked 5% phenylmethylsilicone gum (film thickness 0.25 μm). Helium was used as the carrier gas at an inlet pressure of 50 kPa. Mass spectra were obtained at 70 eV. The split mode was used for injections.

High-Performance Liquid Chromatography (HPLC). Separations were carried out on a Supelcosil LC-8-DB column (25 × 1 cm; particle size 5 μm; Supelco) with a Varian Model 5560 liquid chromatograph. The solvents were (A) 1% acetonitrile in water and (B) 5% acetonitrile in water. The elution program was as follows: solvent A for 35 min and then a linear gradient to 80% B for 25 min followed by a linear gradient to 100% B for 10 min. The flow rate was 3 mL/min, and the column temperature was 30 °C. Fractions containing the desired compounds were collected, lyophilized, and redissolved in 0.2 mol/L DCl in D_2O for measurements by NMR spectroscopy. A small portion of the lyophilized sample was also used for GC–MS analysis.

NMR Spectroscopy. Spectra were acquired by use of the Bruker DISR87 program (version 870101.1) with a Bruker Instruments Model WM-400 spectrometer that was equipped with an Aspect 3000 data system and process controller. The HPLC fractions and reference compounds (≈1 mg for ^1H NMR, 10–15 mg for ^{13}C NMR) were examined as their solutions in 0.2 mol/L DCl (0.6 mL), with TSP added as an internal reference, for both ^1H and ^{13}C NMR spectroscopy (5-mm sample tubes). ^1H NMR spectra were recorded by use of a 30° pulse (3 μs), a spectral width of 4 kHz, 64–240 scans (reference compounds) or 500–15 000 scans (HPLC fractions), and 16 384 data points, with application of a 0–1-Hz line broadening. ^1H-decoupled ^{13}C NMR spectra were acquired by use of a 45° pulse (4.8–6.0 μs), a spectral width of 21.7 kHz, 1000–14 260 scans (reference compounds) or 114 120–286 525 scans (HPLC fractions), and 16 384 data points, with use of a 1–4-Hz line broadening. ^1H-coupled ^{13}C NMR spectra were obtained with NOE (gated decoupling), and the 16 384 point data sets were subjected to Gaussian filtering with a −1.5-Hz line broadening and a Gaussian broadening fraction of 0.3 before being zero filled to 32 768 points prior to FT. Two-dimensional, heteronuclear CH chemical shift correlated ^{13}C NMR spectra were obtained with 4096 (t_2) × 256 (t_1) point data sets, zero-filled to 512 points in the t_1 dimension, 16 or 64 scans/spectrum with two dummy scans, spectral widths of 1.8 and 15.2 kHz in the F_1 and F_2 dimensions, respectively, and ^1H decoupling in both dimensions. The average delay periods $1/2J(CH)$ 3.33 ms and $1/4J(CH)$ 1.67 ms were used.

High-Resolution Mass Spectrometry. Exact masses were measured by peak matching on a Varian MAT 731 mass spectrometer at resolutions of 9000–15 000 and an ion source temperature of 200 °C. Samples were introduced by direct probe.

Results

Analysis of Products by GC–MS. To determine the chemical nature of OH radical induced DNA–protein cross-links in either isolated DNA–protein complexes (e.g., chromatin) or living cells, these products must be hydrolyzed so that a sensitive and selective technique such as GC–MS can be applied to the identification of the actual components of the cross-linked products, as was done in earlier studies of model systems (Dizdaroglu, 1984). The simplest method for hydrolysis appears to be the standard method of protein hydrolysis in hot 6 mol/L HCl; however, it is not known whether Thy–Tyr cross-links (or any other possible base–amino acid cross-links) are stable under such strongly acidic conditions. In the previous work, it was shown that the majority of Thy–Tyr cross-links dehydrate on somewhat milder acidic treatment (i.e., 1 mol/L HCl) and yield one major product, which is comprised of Thy and Tyr moieties, according to the mass spectrum of its Me_3Si derivative (Dizdaroglu, 1984). However, the exact structure of this compound has not been established. Cross-linking between Thy and Tyr has been found to be a major process with a G value of 0.1 μmol (J of radiation energy)$^{-1}$ (Simic & Dizdaroglu, 1985). In the present work, mixtures of Thy and Tyr that had been exposed to OH radicals were treated with 6 mol/L HCl and then trimethylsilylated and analyzed by GC–MS. Figure 1 illustrates a representative total-ion chromatogram from such samples. Peaks 1 and 2 represent Me_3Si derivatives of Thy and Tyr, respectively. Peaks 3 and 4 correspond to Me_3Si derivatives of 2-hydroxytyrosine and DOPA, respectively, which are OH radical induced monomeric products of Tyr. Peak 5 represents the Me_3Si derivative of a Thy–Tyr cross-link. No other compound, which would correspond to a Thy–Tyr cross-link, was observed. Peaks 6–8 were assigned as Me_3Si derivatives of various Tyr dimers on the basis of their mass

[2] Identification of any commercial products or equipment does not imply recommendation or endorsement by the National Bureau of Standards, nor does it imply that the material or equipment identified is necessarily the best for the purpose.

Table I: ^{1}H Chemical Shifts[a] of Tyr Dimer, Thy–Tyr Cross-Link, and Related Compounds

		tyrosines					
proton	DOPA	ortho	meta	para	3,3′ Tyr dimer	Thy–Tyr cross-link	Thy
H-α	4.315	4.420	4.370	4.326	4.360	4.302	
H-β	3.114	3.171	3.186	3.171	3.216	3.151	
H-β	3.240	3.406	3.318	3.288	3.341	3.237	
H-2	6.835		6.822	7.203	7.153	7.055	
H-3		6.940		6.900			
H-4		7.262	6.873				
H-5	6.903	6.952	7.303	6.900	7.019	6.912	
H-6	6.746	7.228	6.887[b]	7.203	7.249	7.091	
Thy H-6′						7.274	7.358
Thy CH_2						3.580	
Thy CH_3							1.855

[a] Measured in ppm by first-order analysis of ^{1}H spectra recorded at 400 MHz. [b] Represents the approximate chemical shift of an unresolved multiplet.

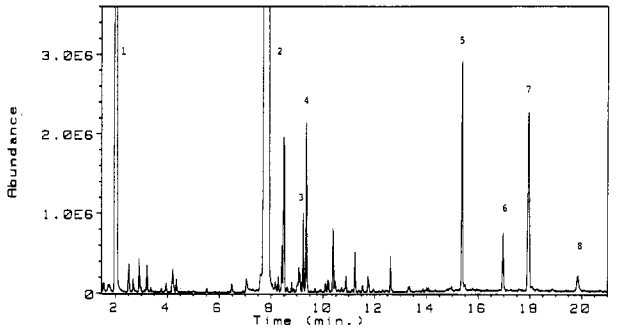

FIGURE 1: Total-ion chromatogram obtained from a γ-irradiated mixture of thymine and tyrosine after treatment with 6 mol/L HCl followed by trimethylsilylation. The column was programmed from 140 to 270 °C at 10 °C/min after 2 min at 140 °C. For other experimental details, see Experimental Procedures.

Scheme I

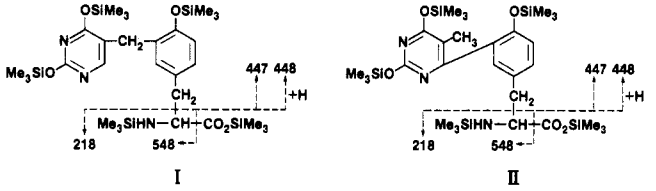

spectra and the data published previously (Karam et al., 1984). No monomeric products of Thy were observed under these experimental conditions, presumably because of their acid-induced decomposition. The origin of peaks not numbered in Figure 1 is unknown.

The mass spectrum taken from the material represented by peak 5 in Figure 1 had characteristic ions at m/z 665 [molecular ion ($M^{\bullet+}$); 1% relative intensity], 650 [$(M - CH_3)^+$; 5%], 622 [$(M - CH_3 - CO)^+$; 2%], 548 (7%), 520 (5%), 448 (100%), 447 (12%), and 218 (18%). This spectrum was identical with that published previously [Figure 17 in Dizdaroglu (1984)]. The suggested structures of two possible isomers and their fragmentation patterns, which would yield the characteristic ions listed above, are shown in Scheme I.

To elucidate the exact structure of this Thy–Tyr cross-link, attempts were made to isolate it by HPLC. Figure 2 illustrates a chromatogram obtained from a mixture of Thy and Tyr, which was exposed to OH radicals and subsequently treated with 6 mol/L HCl. Peaks 1 and 2 represent Tyr and Thy, respectively. Compounds eluting later than Thy (peaks 3 and 4 in Figure 2) were isolated by collection of corresponding fractions, lyophilized, and subsequently analyzed by GC–MS after trimethylsilylation. The compound represented by peak 3 was found to be a dimer of Tyr on the basis of its mass spectrum. A total-ion chromatogram obtained from the compound represented by peak 4 in Figure 2 revealed one

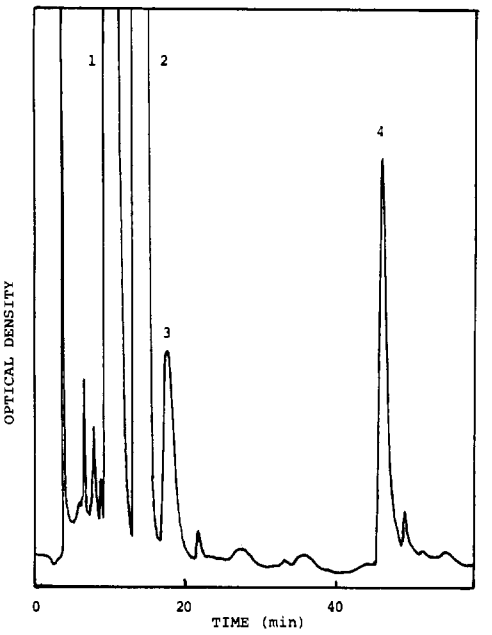

FIGURE 2: HPLC chromatogram of a γ-irradiated mixture of thymine and tyrosine after treatment with 6 mol/L HCl. Sample was 0.5 mg of the irradiated mixture of Tyr and Thy in 10 μL 0.2 mol/L HCl; absorbance was measured at 270 nm at 0.008 AUFS. For other experimental details, see Experimental Procedures.

component together with small amounts of some impurities. The retention time of the single major peak was the same as that of peak 5 in Figure 1. In addition, the mass spectrum taken from this major peak was identical with that taken from peak 5 in Figure 1. Thus it was concluded that peak 5 in Figure 1 and peak 4 in Figure 2 represent the same Thy–Tyr cross-link. Subsequently, this compound (peak 4 in Figure 2) and the Tyr dimer (peak 3 in Figure 2) were isolated by collection of corresponding fractions and then subjected to analysis by ^{1}H and ^{13}C NMR spectroscopy.

Analysis of Product Structures by ^{1}H and ^{13}C NMR Spectroscopy. The assignment of the structure of the Thy–Tyr cross-link was approached by first examining its ^{1}H and ^{13}C NMR spectra. The validity of the assignment of the Thy–Tyr bond is further supported by the similarity of the ^{1}H and ^{13}C NMR chemical shifts of the Tyr moiety to those of the bilaterally symmetrical 3,3′ Tyr dimer. The chemical shifts of the standards and isolated compounds are listed in Tables I and II.

Structure of the Thy–Tyr Cross-Link. The ^{1}H NMR spectrum (Figure 3) of the material represented by peak 4 (Figure 2), which was identified by GC–MS as a Thy–Tyr cross-link, contains seven distinct resonances (Table I). Four

Table II: ^{13}C Chemical Shifts[a] of Tyr Dimer, Thy–Tyr Cross-Link, and Related Compounds

		tyrosines					
carbon	DOPA[b]	ortho	meta[c]	para	3,3′ Tyr dimer	Thy–Tyr cross-link	Thy
COOH	174.4	174.9	174.7	174.3	174.2	174.2	
C-α	57.1	56.6	57.2	57.1	57.1	57.0	
C-β	37.8	33.8	38.5	37.7	37.6	37.7	
C-1	129.3	124.0	138.9	128.6	128.6[d]	128.8[d]	
C-2	120.6	157.4	119.1	133.8	135.2[e]	134.2[e]	
C-3	147.2	118.6	158.9	118.9	128.9[d]	128.7[d]	
C-4	146.6	132.5	117.8	158.1	155.7	156.3	
C-5	119.6	123.7	133.6	118.9	119.4	119.3	
C-6	124.9	134.7	124.4	133.8	133.5[e]	132.1[e]	
CH_3							14.2
CH_2						29.2	
C-2′						183.8	156.1
C-4′						169.7	170.6
C-5′						115.3	113.0
C-6′						143.2	142.0

[a] Measured in ppm at 100.6 MHz. Assignments for the protonated carbons of the Tyr reference derivatives were confirmed by two-dimensional heteronuclear CH chemical shift correlation spectroscopy, performed with ^1H decoupling in both dimensions. The known ^1H NMR assignments of these derivatives were used as the basis for the heteronuclear chemical shift correlations. [b] The assignments for C-3 and C-4 were made from the resolution-enhanced, ^1H-coupled ^{13}C NMR spectrum (with NOE), analysis of which yielded the following coupling constants (Hz): $^1J_{C\text{-}\alpha,H\text{-}\alpha} = 147.8$, $^2J_{C\text{-}\alpha,H\text{-}\beta} = 4.3$, $^1J_{C\text{-}\beta,H\text{-}\beta} = 132.1$, $^2J_{C\text{-}\beta,H\text{-}\alpha} \sim {}^3J_{C\text{-}\beta,H\text{-}2} \sim {}^3J_{C\text{-}\beta,H\text{-}6} \sim 4.3$, $^3J_{C\text{-}1,H\text{-}\alpha} \sim {}^2J_{C\text{-}1,H\text{-}\beta} \sim 4.9$, $^3J_{C\text{-}1,H\text{-}5} = 9.6$, $^1J_{C\text{-}2,H\text{-}2} = 156.4$, $^3J_{C\text{-}2,H\text{-}\beta} \sim {}^3J_{C\text{-}2,H\text{-}6} \sim 6.0$, $^2J_{C\text{-}3,H\text{-}2} = 2.7$, $^3J_{C\text{-}3,H\text{-}5} = 7.3$, $^3J_{C\text{-}4,H\text{-}2} = 9.3$, $^2J_{C\text{-}4,H\text{-}5} = 2.5$, $^3J_{C\text{-}4,H\text{-}6} = 6.8$, $^1J_{C\text{-}5,H\text{-}5} = 160.2$, $^1J_{C\text{-}6,H\text{-}6} = 160.9$, $^3J_{C\text{-}6,H\text{-}\beta} \sim {}^3J_{C\text{-}6,H\text{-}2} \sim 5.9$, and $^2J_{C=O,H\text{-}\alpha} \sim {}^3J_{C=O,H\text{-}\beta} \sim 4.1$ Hz. [c] Assignments were made from the resolution-enhanced, ^1H-coupled ^{13}C NMR spectrum (with NOE), analysis of which gave the following coupling constants (Hz): $^1J_{C\text{-}\alpha,H\text{-}\alpha} = 147.6$, $^2J_{C\text{-}\alpha,H\text{-}\beta} = 4.6$, $^1J_{C\text{-}\beta,H\text{-}\beta} = 132.1$, $^2J_{C\text{-}\beta,H\text{-}\alpha} \sim {}^3J_{C\text{-}\beta,H\text{-}2} \sim {}^3J_{C\text{-}\beta,H\text{-}6} \sim 4.4$, $^3J_{C\text{-}1,H\text{-}\alpha} \sim {}^2J_{C\text{-}1,H\text{-}\beta} \sim 4.9$, $^3J_{C\text{-}1,H\text{-}5} = 9.5$, $^1J_{C\text{-}2,H\text{-}2} = 157.2$, $^3J_{C\text{-}2,H\text{-}\beta} \sim {}^3J_{C\text{-}2,H\text{-}4} \sim {}^3J_{C\text{-}2,H\text{-}6} \sim 5.5$, $^3J_{C\text{-}3,H\text{-}\beta} = 10.0$, $^1J_{C\text{-}4,H\text{-}4} = 160.3$, $^3J_{C\text{-}4,H\text{-}2} = 7.6$, $^3J_{C\text{-}4,H\text{-}6} = 4.7$, $^1J_{C\text{-}5,H\text{-}5} = 160.5$, $^1J_{C\text{-}6,H\text{-}6} = 160.2$, $^3J_{C\text{-}6,H\text{-}\beta} \sim {}^3J_{C\text{-}6,H\text{-}2} \sim {}^3J_{C\text{-}6,H\text{-}4} \sim 6.0$, and $^2J_{C=O,H\text{-}\alpha} \sim {}^3J_{C=O,H\text{-}\beta} \sim 4.2$ Hz. [d] Assignments may be interchanged. [e] Assignments may be interchanged.

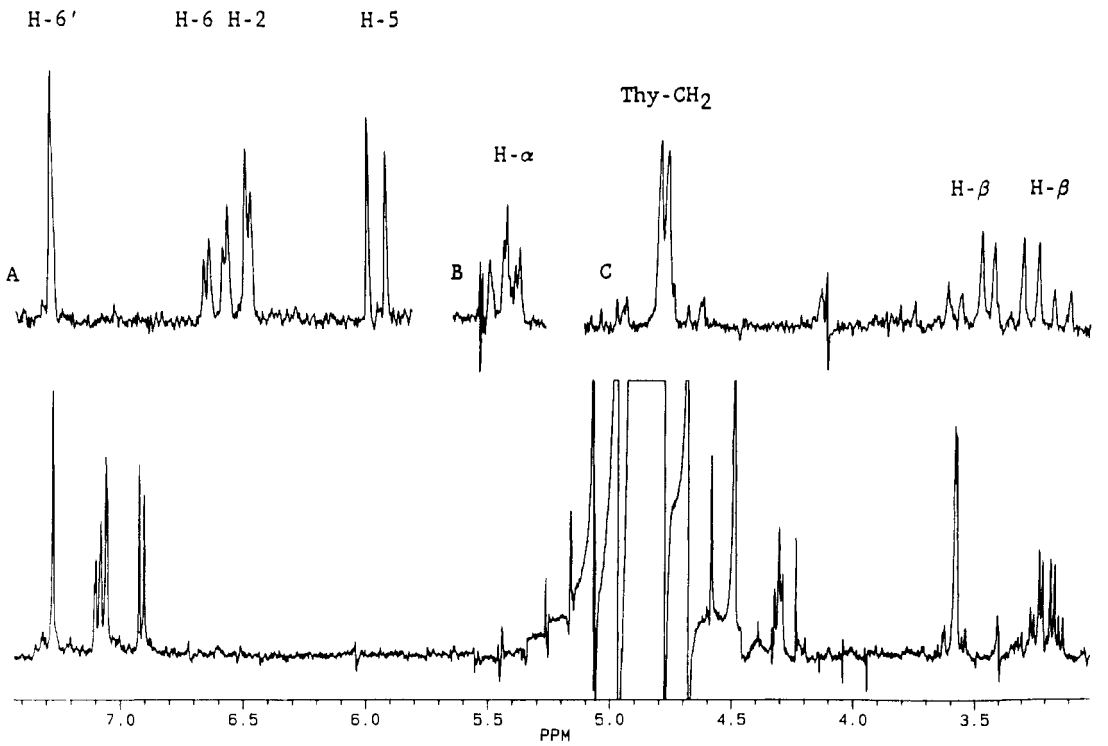

FIGURE 3: The 400-MHz FT ^1H NMR spectrum of Thy–Tyr cross-link (peak 4, Figure 2). The lyophilized dimer was dissolved in 0.6 mL of 0.2 mol/L DCl in D_2O. The spectrum was recorded at 27 °C with TSP as the internal standard. (A) Expanded aromatic region. (B) Expanded α-proton region. (C) Expanded β-proton and Thy methylene proton region.

of these signals (6.912, 7.056, 7.091, and 7.274 ppm) are of aromatic nature. Two of the other three signals exhibit splitting and chemical shifts characteristic of the α- and β-protons of the amino acid. The third resonance has a chemical shift (3.580 ppm) which is characteristic of a methylene bridge between two aromatic rings. The areas of each of the four aromatic resonances and the α-proton are equal and half the area of the resonance of the β-proton and the methylene protons. This accounts for all of the protons of the molecule and suggests that this cross-link resulted from the formation of a covalent bond between the tyrosine ring and the thymine molecule. The absence of a methyl signal (1.855 ppm in the case of thymine) and the presence of the methylene bridge resonance (3.580 ppm) of the proper area indicate that the cross-linking involved the methyl group of thymine. The singlet at 7.274 ppm is assigned to H-6 of the Thy moiety of the Thy–Tyr cross-link (compare 7.358 ppm for Thy), and it is not coupled to any other nonexchangeable proton. The existence of this characteristically deshielded proton on Thy C-6 eliminates this carbon atom as a site of cross-linking. The other three resonances in the aromatic proton region are two doublets and a doublet of doublets, namely, doublet 1 with a

Table III: ^1H–^1H Coupling Constants[a] (Hz) for Tyrosine Isomers and Tyrosine-Containing Dimers

compound	$J_{2,3}$	$J_{2,4}$	$J_{2,6}$	$J_{3,4}$	$J_{3,5}$	$J_{4,5}$	$J_{4,6}$	$J_{5,6}$	$J_{\alpha,\beta}$	$J_{\alpha,\beta}$	$J_{\beta,\beta}$
o-Tyr				~7.5	~1.3	8.0	~1.6	7.9	5.4	7.6	14.5
m-Tyr		2.5	1.6			7.9	0.7	7.9	5.6	7.6	14.6
p-Tyr	8.1							8.1	5.6	7.5	14.7
DOPA			2.0					8.1	5.5	7.5	14.7
3,3′ Tyr dimer			2.2					8.3	5.7	7.5	14.8
Thy–Tyr			2.3					8.2	5.9	7.3	14.8

[a] First-order analysis of ^1H NMR spectra recorded at 400 MHz.

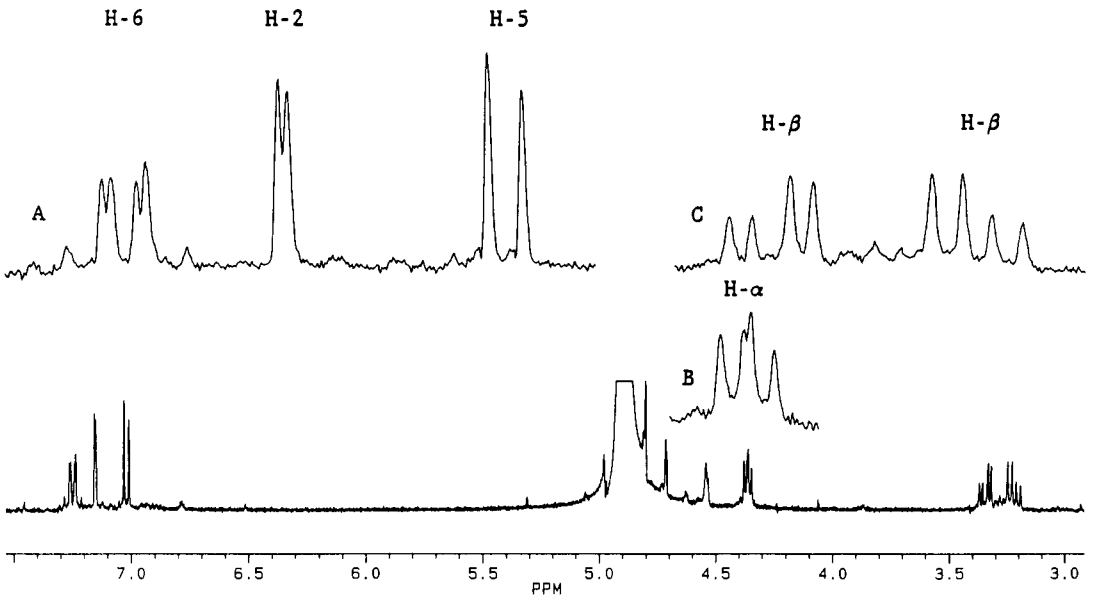

FIGURE 4: The 400-MHz FT ^1H NMR spectrum of 3,3′ Tyr dimer (peak 3, Figure 2). The lyophilized dimer was dissolved in 0.6 mL of 0.2 mol/L DCl in D_2O. The spectrum was recorded at 27 °C with TSP as the internal standard. (A) Expanded aromatic region. (B) Expanded α-proton region. (C) Expanded β-proton region.

coupling constant of 8.2 Hz, doublet 2 with a coupling constant of 2.3 Hz, and a doublet of doublets with coupling constants of 2.3 and 8.2 Hz (Table III). The large coupling constant of 8.2 Hz indicates that this proton of doublet 1 is coupled to a vicinal proton that is represented by the doublet of doublets that has a similar coupling constant. The additional splitting observed in the doublet of doublets is caused by long-range coupling to a meta proton. The remaining proton, which has only a small coupling constant of 2.3 Hz, cannot have a proton in an ortho relationship; otherwise, it would have a coupling constant of about 8 Hz. Therefore, this proton must be meta to one of the other two protons. Furthermore, these coupling constants are consistent with those observed for 1,3,4-trisubstituted benzenes (see DOPA, Table III). The α- and β-protons of the Tyr side chain exhibit splitting patterns and coupling constants which are very similar to those of the Tyr standards and which are characteristic of the aromatic amino acids (Table I and III). The ratio of the areas of these proton signals to the area of any one of the aromatic proton signals is 1:2:1. Decoupling of the α-proton led only to collapse of the signals of the β-protons from a doublet of quartets to a single quartet. The location of the third aromatic proton of Tyr and the cross-linking site can be established definitively with the aid of the ^{13}C NMR spectrum. This ^{13}C NMR spectrum contains 14 resonances which are consistent with a Thy–Tyr cross-link (Table II). Examination of the chemical shifts and intensities of the resonances at low field indicates the presence of four protonated carbons at 119.3, 132.1, 134.2, and 143.2 ppm; four quaternary carbons at 115.3, 128.8, 128.7, and 156.3 ppm; two NC-type carbons at 169.7 and 183.8 ppm; and a $-CO_2H$ at 174.2 ppm. These assignments are consistent with the chemical shifts of the reference materials (Table II). Examination of the resonances of the dimer indicates that one of the protonated Tyr carbons (119.3 ppm) is more shielded than the others and is therefore adjacent to the hydroxylated carbon. The other two protonated carbons (132.1 and 134.2 ppm) are less shielded and are therefore more remote from the hydroxyl carbon, indicating that dimerization occurred at C-3 of the tyrosine ring. The assignment of these ^{13}C signals is consistent with the assignment of the protonated aromatic carbons of the 3,3′ dimer of Tyr. The presence of the pyrimidine carbon resonances at 183.8 (C-2′), 169.7 (C-4′), 115.3 (C-5′), and 143.2 (C-6′) ppm; the absence of the methyl signal in the region of 14.2 ppm (the chemical shift of the methyl carbon of the thymine monomer); and the appearance of a methylene carbon signal at 29.2 ppm prove that the cross-linking of Thy with Tyr occurred between the methyl carbon of Thy and C-3 of the aromatic ring of Tyr.

Structure of Tyr Dimer. The ^1H and ^{13}C NMR spectra of the 3,3′-Tyr dimer have been examined in detail because the ^1H chemical shifts (Table I) and coupling constants (Table III) and the ^{13}C chemical shifts (Table II) of this bilaterally symmetrical molecule are very similar to those of the Tyr moiety of the Thy–Tyr cross-link. These results support the assignments of the chemical shifts for the Tyr moiety of the Thy–Tyr cross-link since the splitting patterns and coupling constants are characteristic of a 1,3,4-trisubstituted benzene (e.g., DOPA; Table III). The ^1H NMR spectrum of the compound represented by peak 3 (Figure 2) is illustrated in Figure 4. This compound has been identified previously as a Tyr dimer, by GC–MS (Karam et al., 1984). The assignment of the signals in the aromatic region is based upon the same rationale as that used for the Thy–Tyr cross-link. The assignment of the signals in the ^{13}C NMR spectra (Table II)

Table IV: Exact Masses of Some Ions from the Mass Spectrum of the Me_3Si Derivative of Thy–Tyr Cross-Link

ion (m/z)	composition	exact mass		resolution
		calcd	measd	
218	$C_8H_{20}NO_2Si_2$	218.1033	218.1032	12000
447	$C_{21}H_{35}N_2O_3Si_3$	447.1956	447.1949	12000
448	$C_{21}H_{36}N_2O_3Si_3$	448.2034	448.2013	12000
548	$C_{25}H_{46}N_3O_3Si_4$	548.2616	548.2615	15000
650	$C_{28}H_{52}N_3O_5Si_5$	650.2754	650.2749	15000
665	$C_{29}H_{55}N_3O_5Si_5$	665.2988	665.2968	9000

was based upon the similarity of their chemical shifts to those of analogous carbons in the Tyr monomers. The fact that the OH group has a shielding effect on only one carbon demonstrates conclusively that the dimer bond connects the C-3's of the aromatic rings. This dimer is identical with the one reported by Gross and Sizer (1959), and these results confirm the observations of Boguta and Dancewicz (1978).

Exact Mass Measurements. The isolated Thy–Tyr cross-link was also analyzed by high-resolution mass spectrometry after trimethylsilylation to ascertain its exact chemical composition and fragmentation pattern, which were suggested in Scheme I. Exact masses of characteristic ions at m/z 218, 447, 448, 548, 650, and 665 were measured. Table IV clearly shows the excellent agreement of the values obtained with the theoretical values of masses calculated on the basis of the compositions of the fragments suggested above.

Discussion

OH radicals react with Thy by addition to the C5-C6 double bond and by H abstraction from the methyl group. The distribution of OH radical attack has been determined recently (Fujita & Steenken, 1981). The addition takes place preferentially at C-5 (60%) and C-6 (30%), and the H abstraction from the methyl group amounts to 10%. Similarly, OH radicals react with Tyr by addition to the aromatic ring to give dihydroxycyclohexadienyl radicals (Dorfman et al., 1962). The preferred sites of attack are at C-3 (~50%) and at C-2 (~35%) (Solar et al., 1984). The C-3 OH radical adduct eliminates water to give a phenoxyl radical (Land & Ebert, 1967). In individual Thy and Tyr systems, the radicals undergo disproportionation and dimerization reactions [for a review, see von Sonntag (1987)]. When both Thy and Tyr are present in the system, cross-linking reactions between Thy radicals and Tyr radicals are expected to take place as well. In fact, this has been observed in a previous work (Dizdaroglu, 1984; Simic & Dizdaroglu, 1985); however, the exact structures of products of cross-linking reactions have not been determined. Some possible mechanisms of formation for the Thy–Tyr cross-link identified in this work are [R represents CH_2–$CH(NH_3^+)CO_2^-$]

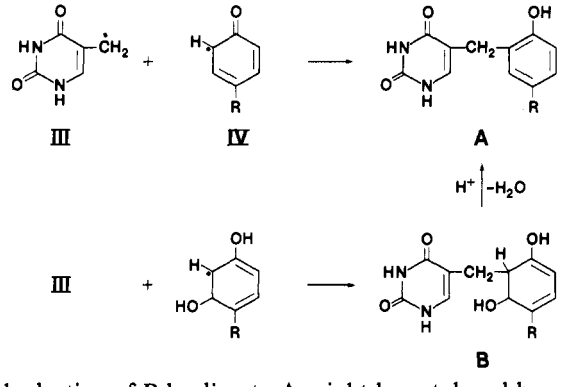

Dehydration of B leading to A might be catalyzed by acidic treatment used in this work. Indeed, dehydration of Thy–Tyr cross-links on acidic treatment has been described previously (Dizdaroglu, 1984). Since A is the only Thy–Tyr cross-link observed in the present work, one of the Thy–Tyr cross-links observed prior to acidic treatment in the previous work (Dizdaroglu, 1984; Simic & Dizdaroglu, 1985) might be B. The mass spectrum of the Me_3Si derivative of B would be consistent in terms of the molecular weight and fragmentation patterns with mass spectra obtained from cross-linked products of Thy and Tyr prior to acidic treatment (Dizdaroglu, 1984). Cross-linking of other Thy radicals with Tyr radicals is also plausible. As an example, the formation of one possible product is

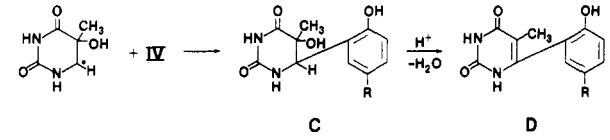

The Me_3Si derivative of D would have the same molecular weight and substantially the same fragmentation patterns as the Me_3Si derivative of A (see structures I and II in Scheme I). However, space-filling models of A and D indicate steric hindrances in D because of the close proximity of the methyl and hydroxyl groups. Steric hindrances should be even more significant in C, which is the precursor of D, because of the presence of the methyl and hydroxyl groups at the C-5 position of the Thy moiety. This means that the formation of products such as C should be less likely than that of A. It is not known at present whether a product such as A would be formed when DNA–protein complexes are exposed to OH radicals in vitro or in vivo. The amount of one of the radical precursors of A formed in aqueous solutions of Thy is relatively small when compared with those of other Thy radicals (Fujita & Steenken, 1981). This ratio might be quite different in a native system such as chromatin. Cross-linking in vivo by combination of a DNA base radical and an amino acid radical may require the formation of two such radicals in close proximity. The likelihood of this process is not known. An alternative mechanism would be the addition of the Thy radical III to the aromatic ring of Tyr and the subsequent oxidation of the adduct radical formed. In any case, the cross-linking of a base to an amino acid in vivo requires the close proximity of participating DNA and protein components. In the case of Thy and Tyr, this appears to be quite likely because Tyr uniquely forms a hydrogen bond between its hydroxyl group and the oxygen at the C-4 position of a neighboring Thy (Hendry et al., 1981). This might permit the close proximity of the methyl group of Thy to the aromatic ring of Tyr.

Clarification of the mechanism of OH radical induced DNA–protein cross-linking in DNA–protein complexes in vitro or in vivo awaits the chemical characterization of the actual cross-linked components of DNA and proteins and of the chemical bonds involved. We hope that the approach presented in this work will open up a route for achievement of this goal.

Acknowledgments

We thank Dr. Edward White V and Jon-Marc Rodier for the exact mass measurements by high-resolution mass spectrometry.

Registry No. DOPA, 59-92-7; 3,3′-Tyr dimer, 980-21-2; *o*-Tyr, 709-16-0; *m*-Tyr, 587-33-7; *p*-Tyr, 60-18-4; OH•, 3352-57-6; thymine, 65-71-4.

References

Boguta, G., & Dancewicz, A. M. (1978) *Stud. Biophys. 73*, 149–156.

Dizdaroglu, M. (1984) *J. Chromatogr. 295*, 103–121.
Dizdaroglu, M., & Simic, M. G. (1985) *Int. J. Radiat. Biol. Relat. Stud. Phys., Chem. Med. 47*, 63–69.
Dorfman, L. M., Taub, I. A., & Buhler, R. E. (1962) *J. Chem. Phys. 36*, 3051–3061.
Fujita, S., & Steenken, S. (1981) *J. Am. Chem. Soc. 103*, 2540–2545.
Gross, A. J., & Sizer, I. W. (1959) *J. Biol. Chem. 234*, 1611–1614.
Hendry, L. B., Bransome, E. D., Jr., Hutson, M. S., & Campbell, L. K. (1981) *Proc. Natl. Acad. Sci. U.S.A. 78*, 7440–7444.
Karam, L. R., Dizdaroglu, M., & Simic, M. G. (1984) *Int. J. Radiat. Biol. Relat. Stud. Phys., Chem. Med. 46*, 715–724.
Land, E. J., & Ebert, M. (1976) *Trans. Faraday Soc. 63*, 1181–1190.
Mee, L. K., & Adelstein, S. J. (1979) *Int. J. Radiat. Biol. Relat. Stud. Phys., Chem. Med. 36*, 359–366.
Mee, L. K., & Adelstein, S. J. (1981) *Proc. Natl. Acad. Sci. U.S.A. 78*, 2194–2198.
Oleinick, N. L., Chiu, S., Friedman, L. R., Xue, L. & Ramakrishnan, N. (1986) in *Mechanisms of DNA Damage and Repair* (Simic, M. G., Grossman, L., & Upton, A. C., Eds.) pp 181–192, Plenum, New York.
Simic, M. G., & Dizdaroglu, M. (1985) *Biochemistry 24*, 233–236.
Smith, K. C. (1976) in *Aging, Carcinogenesis and Radiation Biology* (Smith, K. C., Ed.) pp 67–81, Plenum, New York.
Solar, S., Solar, W., & Getoff, N. (1984) *J. Phys. Chem. 88*, 2091–2095.
von Sonntag, C. (1987) *The Chemical Basis of Radiation Biology*, Taylor & Francis, London.
Yamamoto, O. (1976) in *Aging, Carcinogenesis and Radiation Biology* (Smith, K. C., Ed.) pp 165–192, Plenum, New York.

Solution Conformations of DNAs Containing Binding Sites of the Catabolite Gene Activator Protein and *lac* Repressor Protein: Characterization by Raman Spectroscopy†

Henry DeGrazia,‡ Daniel Brown,‡ Susannie Cheung,§ and Roger M. Wartell*,‡

Schools of Physics and Applied Biology, Georgia Institute of Technology, Atlanta, Georgia 30332, and Department of Chemistry, University of Pennsylvania, Philadelphia, Pennsylvania 19104

Received January 19, 1988; Revised Manuscript Received April 25, 1988

ABSTRACT: Raman spectra from three subfragments of the *Escherichia coli* lactose promoter region were obtained in 0.1 M NaCl. The three DNAs are 21, 40, and 62 bp in length. The 21 and 62 bp DNAs contain the binding site for the catabolite gene activator protein (CAP). The 40 bp DNA contains the binding site for the *lac* repressor. A quantitative analysis of Raman band characteristics indicates an overall B-type conformation for these gene regulatory sites. Bands which correspond to A-family (807 cm^{-1}) and B-family (834 cm^{-1}) deoxyribose phosphate vibrations have the same intensities as bands found in heterogeneous DNAs. The spectra of the 21 bp CAP site have, however, a small band at 867 cm^{-1} and several other small differences similar to some characteristics observed in C-DNA spectra. Several dG nucleosides in the CAP site appear to be altered from the conventional C2′-endo/anti conformation. At 45 °C, well below the melting region of these DNAs, small changes occur in the spectra of the 40 bp *lac* repressor site which are not observed in the other DNAs. A weak band occurs at 705 cm^{-1}, and intensity changes are observed at 497, 682, and 792 cm^{-1}. The changes suggest that the conformations of several dG nucleosides are altered and that a small region may exist with characteristics of an A-family backbone. This conformational change at 45 °C coincides with previous NMR observations indicating an enhanced imino proton exchange rate at a GTG sequence within the *lac* operator site.

Crystal structures of DNA duplex oligomers (Wing et al., 1980; Kopka et al., 1983; Brown et al., 1986) and solution studies (Nilges et al., 1987; Prescott et al., 1985) have demonstrated that local structural variations can occur within a B-family DNA structure. These structural variations appear to depend upon base pair sequence. The ability of a DNA sequence to adopt specific conformations may play several roles in the selective interaction between a gene regulatory protein and its DNA site. The spatial location of chemical groups on DNA will affect the initial interaction between a protein and DNA site. DNA sequence may also influence a protein-induced alteration in DNA secondary structure (Hogan & Austin, 1987). How base pair sequence and environment influence DNA structure, particularly in solution, is not well understood (Dickerson, 1987).

We present in this report a Raman spectroscopic study on DNA molecules which contain protein binding sites within the *Escherichia coli* lactose promoter. Three DNA fragments, 62, 40, and 21 bp, were examined. The 21 and 62 bp DNAs contain the binding region of the catabolite gene activator protein, CAP (also known as cAMP receptor protein, CRP). The 40 bp DNA contains the binding site of the *lac* repressor. Previous ^1H NMR studies on the latter DNA indicated that

† This work was supported by NIH Grant GM 33543.
* Author to whom correspondence should be addressed.
‡ Georgia Institute of Technology.
§ University of Pennsylvania.

0006-2960/88/0427-6359$01.50/0